Methods to Evaluate Land-Atmosphere Exchanges in Amazonia Based on Satellite Imagery and Ground Measurements

Gabriel de Oliveira, Nathaniel A. Brunsell,
Elisabete C. Moraes, Yosio E. Shimabukuro,
Guilherme A. V. Mataveli, Thiago V. dos Santos,
Celso von Randow and Luiz E. O. C. Aragao

Additional information is available at the end of the chapter

Abstract

During the last three decades, intensive campaigns and experiments have been conducted for acquiring micrometeorological data in the Amazonian ecosystems, which has increased our understanding of the variation, especially seasonally, of the total energy available for the atmospheric heating process by the surface, evapotranspiration and carbon exchanges. However, the measurements obtained by such experiments generally cover small areas and are not representative of the spatial variability of these processes. This chapter aims to discuss several algorithms developed to estimate surface energy and carbon fluxes combining satellite data and micrometeorological observations, highlighting the potentialities and limitations of such models for applications in the Amazon region. We show that the use of these models presents an important role in understanding the spatial and temporal patterns of biophysical surface parameters in a region where most of the information is local. Data generated may be used as inputs in earth system surface models allowing the evaluation of the impact, both in regional as well as global scales, caused by land-use and land-cover changes.

Keywords: surface energy budget, CO_2 fluxes, eddy covariance, remote sensing, Amazon region

1. Introduction

Amazon rainforests directly influences the terrestrial climate system due to the emission or absorption of carbon dioxide (CO_2) and evapotranspiration (ET), that is, through the processes of transpiration of plants and evaporation of water contained in leaves, stems, litter and soil [1, 2]. In addition to providing water vapor to the environment, influencing the general circulation in the tropics and contributing to regional precipitation, the Amazon rainforests are important in the atmospheric carbon cycle [3, 4]. Consequently, deforestation in the Amazon can lead to changes in surface net radiation (R_n), resulting in higher or lower availability of energy for the evapotranspiration processes and in the amount of CO_2 absorbed or released by the atmosphere [5–7].

The relevance of physical phenomena related to energy exchanges between the surface and atmosphere under climate change leads to the need for improving studies on both temporal as well as spatial scales [8, 9]. During the last three decades, intensive campaigns and experiments have been developed for acquiring micrometeorological data in the Amazonian ecosystems, which has increased our understanding of the variations, especially seasonally, of the total energy available for the atmospheric heating process by the surface, ET and atmospheric CO_2 exchanges [10, 11]. However, measurements obtained by such experiments are usually local and representative of small areas, and therefore not representative of the spatial variability of these processes [12, 13].

In this context, new methodologies have been developed to obtain the components related to energy and CO_2 exchanges between the surface and atmosphere, such as the use of remote sensing (RS). Usually, the use of orbital sensors to estimate energy and CO_2 fluxes are performed using models that consider information obtained directly from the satellite images as inputs, such as reflectance and land surface temperature (LST) [14, 15]. Regarding the estimation of surface energy fluxes, several algorithms have been developed, such as the Simplified Surface Energy Balance Index (S-SEBI) [16] and Evapotranspiration Assessment from Space (EVASPA) [17]. To estimate CO_2 fluxes, we can highlight Parametric Production Efficiency Model (C-Fix) [18] and Temperature and Greenness Rectangle Model (TGR) [19]. These models were applied in different terrestrial biomes; however, it is worth mentioning that in the Amazon region such approach for the determination of energy and CO_2 fluxes using RS data is still incipient [20–25].

Based on the considerations above, this chapter aims to present and discuss several models developed to estimate surface energy and CO_2 fluxes by combining satellite data and micrometeorological observations, highlighting the potentialities and limitations of such models for applications in the Amazon region.

2. Biosphere-atmosphere interactions studies in the Amazon region using in-situ measurements

Since the 1980s, a series of micrometeorological experiments have been conducted in the Amazon region aiming to better understand the interactions between the rainforests and

the atmosphere (i.e. Amazonian Research Micrometeorological Experiment (ARME, 1983–1985) [26], Amazonian Boundary-Layer Experiment (ABLE, 1985–1987) [27], Anglo-Brazilian Amazonian Climate Observational Study (ABRACOS, 1991–1995) [28], and Green Ocean Amazon Experiment (GO-AMAZON, 2014–2015) [29]). Currently, the main source of surface measurements in the region is the Large-Scale Biosphere-Atmosphere Experiment in Amazonia (LBA) [30]. LBA has sites on different land-use locations in the states of Rondonia (RO), Amazonas (AM), Para (PA) and Tocantins (TO). LBA data have been used to analyze the current state of the Amazonian ecosystem, as well as to serve as input and validation parameters for climate prediction numerical models [31].

Typical variables collected at these surface experiments are incoming solar radiation (K↓), outgoing solar radiation (K↑), albedo (α_s) [32, 33], incoming (L↓) thermal infrared (TIR) radiation, emitted TIR (L↑), net radiation (R_n) [34, 35], soil heat flux (G), sensible heat flux (H), latent heat flux (λE) [10, 36], and the net ecosystem exchange (NEE) [5, 37]. It is important to mention that most of the observational studies in the Amazon region have been performed over primary forest and pasture areas. In this context, one way to extend such analyses to the diverse ecosystems of the Amazon is the combined use of surface measurements (i.e. plot-level and flux towers biometric studies) and RS data [38, 39].

3. Modeling energy and CO_2 fluxes combining remote sensing and ground data

The frequency at which satellite data are obtained and processed, combined with the possibility of regional and global studies, provides an excellent cost-benefit ratio. In recent years, there has been a gradual advance in the technical characteristics of the sensors onboard orbital platforms, which present increasingly improved spatial, temporal, radiometric, and spectral resolutions. Within this context, the scientific community has used orbital data to estimate surface biophysical and hydrological parameters using different algorithms. Focusing on the estimation of energy and CO_2 fluxes using RS and ground observations, this topic presents the main models available in the literature that can be applied in the Amazon region.

3.1. Models to estimate energy fluxes

First studies to estimate energy fluxes using RS date back to the 1970s [40], driven by the limited spatial density of surface measurements, which prevented more robust large-scale studies [41]. Currently, studies are focused not only in the estimation but also on describing the land-vegetation-atmosphere energy exchange processes in order to better understand, for example, the feedback mechanisms between the surface and the boundary layer. This issue is gaining importance due to potential climate change [42].

Energy fluxes models differ according to the input data, assumptions and accuracy of the results [43, 44]. However, a common aspect among the algorithms is the orbital input data, once all algorithms require information regarding the visible, near infrared and thermal infrared spectral regions. The primary estimates from such models are related to R_n, G, H, λE and,

consequently, ET. ET is considered a key variable in such models, and, likewise, the most complex variable when referring to the accurate estimate. **Figure 1** [25] exemplifies ET estimates in the Amazon region obtained through MODIS images. Briefly, according to Ruhoff et al. [45], such algorithms are based on (1) empirical and statistical methods, (2) residual energy balance methods, and (3) other physical methods (i.e. Penmann-Monteith equation [46]).

3.1.1. Surface energy balance algorithms for land (SEBAL)

SEBAL [47] is a model based on empirical relationships and physical parametrizations. It was developed to estimate the energy available at surface using daily orbital data and minimal field measurements. Input variables are related to air temperature and wind speed during the satellite passing. SEBAL has been improved since its conception, for example, with the addition of new parametrizations such as those for α_s [48], and G [49].

The algorithm consists of several steps, with R_n being the first component of the energy balance to be obtained. Following $R_{n'}$ it is possible to estimate G (as a function of $R_{n'}$ normalized difference
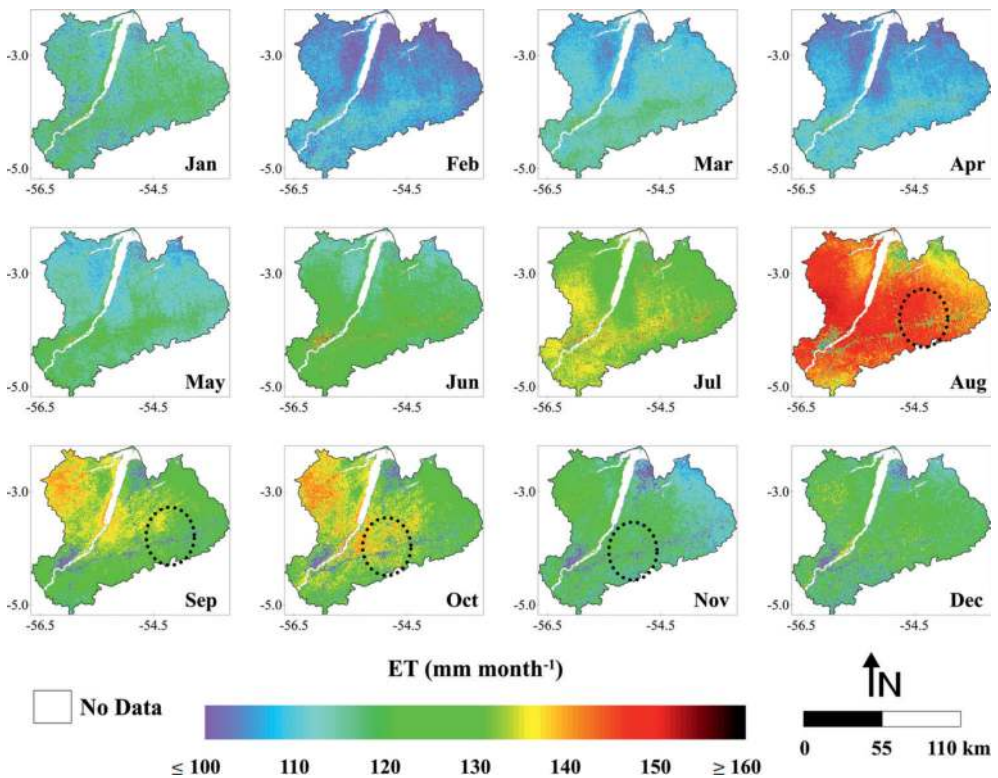

Figure 1. Obtained from the study of De Oliveira et al. [25]. Monthly averages of evapotranspiration (ET) (mm month^{-1}), between the years 2001 and 2006, in the eastern flank of the Amazon region, using MODIS images. The black dashed circles show the spatial pattern of deforestation in the Amazon, known as the fish bone.

vegetation index (NDVI), α_s, and land surface temperature (LST)), and H, which requires the determination of pixels representing extreme conditions of temperature and humidity in the study area, referred to as hot and cold pixels. The determination of hot and cold pixels is an issue, where the lack of user-experience can introduce errors, such as defining fire pixels as hot pixels and cloud pixels as cold pixels [50]. Recent studies proposed statistical approaches to automatically select hot and cold pixels [51]. One of the last steps of SEBAL is the estimation of daily actual ET (ET$_{r24h}$):

$$ET_{r_{24h}} = 86400 \frac{\Lambda R_{n24h}}{\lambda} \tag{1}$$

where Λ is the evaporative fraction, R_{n24h} is the average daily radiation budget, and λ corresponds to the latent heat of water vaporization ($\lambda = 2.45 \times 10^6$ J Kg^{-1}).

SEBAL has been applied and validated in different regions [14, 52–54]. This model is sensitive to land-use, allowing for evaluations in agricultural areas, deserts, prairies, and forests [55, 56]. Regarding the accuracy of the estimates, studies indicate relative errors ranging between ~5 and 17% [14, 57–59]. The error variation was mostly related to the spatial resolution of the satellite images used. Also, it should be highlighted that the main sources of uncertainties in SEBAL are related to the determination of H and the low sensitivity of the model to soil moisture and water stress [47].

Studies using SEBAL have been conducted in the Amazon region, such as in De Oliveira and Moraes [21], De Oliveira et al. [22], Liberato et al. [60], Santos et al. [61], and Ferreira et al. [62]. These studies were performed in the southwestern and eastern parts of the Amazon using LBA data from the following sites: Fazenda Nossa Senhora Aparecida (FNSA) (RO), Reserva Biologica do Jaru (RBJ) (RO), Floresta Nacional de Caxiuana (CAX) (PA), and Floresta Nacional do Tapajos (FNT) (PA). Orbital input data were acquired from the Moderate Resolution Imaging Spectroradiometer (MODIS) sensors onboard Terra and Aqua satellites and the Thematic Mapper (TM) sensor onboard LANDSAT-5. Results found for Rn were satisfactory, presenting relative errors of ~1–16%. For ET, the errors were higher, in the order of ~25%. It should be noted that such studies were conducted over relatively small/medium areas (~7500.000 hectares) and some of them covered only pixels where the flux towers were located due to the difficulty in acquiring cloud free images.

A possible way to operationalize SEBAL for larger scale studies in the Amazon region is using data from 8 or 16 days composites or monthly images from MODIS sensor [63], in which cloud cover effects are attenuated. Although considering that the algorithm was developed for daily images, difficulties emerge related to the surface input data, which need to be acquired during the satellite crossing. In this regard, we highlight the study conducted by De Oliveira et al. [22], in which an approach was developed to estimate R_n and its components under all-sky conditions for the Amazon region through SEBAL model utilizing only RS and reanalysis data. Comparison between estimates obtained by the proposed method and observations from LBA towers showed errors between ~13–16% and ~11–16% for instantaneous and daily R_n, respectively. According the authors, the approach was an alternative to minimize the problem related to strong cloudiness over the region and allowed for consistently mapping the spatial distribution of net radiation components in Amazonia. In this regard, we highlight that further studies should focus in the determination of ET, the most important component of the Amazon hydrological balance.

3.1.2. Simplified surface energy balance index (S-SEBI)

S-SEBI [16] is a semi-empirical model developed soon after SEBAL, such that both models are very similar. The main differences between both models are related to the estimation of thermal infrared radiation emitted from the surface, H and λE [64], which will be discussed further. S-SEBI needs spectral radiance orbital data obtained during clear sky conditions from visible, near infrared and thermal infrared spectral regions to define the initial variables of the model, which are the reflectance, LST and vegetation indices. From these initial variables and the inclusion of air temperature data, it is possible to estimate all the energy balance terms [65, 66].

R_n is estimated from the residual term of solar radiation and thermal infrared exchanges, and G is estimated from the empirical relationship between the characteristics of the surface and the vegetation [67]. It is important to highlight that G is one of the components of the energy balance equation most difficult to be accurately estimated using RS data. Therefore, regardless of the parametrization or the model applied, the equation to obtain G must be adjusted locally in order to achieve better results [68]. It is important to mention here that in forested areas such variable is not relevant to the energy balance; however, over bare soil or areas with sparse vegetation G is an important component of the energy balance.

H and λE are estimated from the evaporative fraction ($\ni$) [16], consisting on the main difference between SEBAL and S-SEBI models [43]. In S-SEBI, sensible and latent heat fluxes are obtained at the same time directly from the $\wedge$, while in SEBAL such variables are estimated separately. Thus, it is not necessary to select pixels representing the null conditions of the fluxes when using S-SEBI. According to Roerink et al. [16], there is a correlation between reflectance and LST in areas presenting constant atmospheric forcings. Therefore, it is assumed that the $\wedge$ varies linearly with LST for a given albedo. By using regressions, it is possible to identify the superior (drier, higher H) and inferior (wetter, higher λE) limits of LST. From the instantaneous values of H and λE, daily ET can be estimated for the entire image.

Studies based on S-SEBI generally use TM/LANDSAT-5 data and are focused on evaluating agricultural areas in Europe and Asia [69–71]. In Brazil, S-SEBI was applied in the semi-arid [72] and in the southwestern regions [73]. Errors found in these studies ranged from ~10 to 30%. It is worth mentioning that S-SEBI usually presents higher errors than those obtained from SEBAL, which, according to Sobrino et al. [67], is related to the more robust estimation of H in the algorithm proposed by Bastiaanssen et al. [57]. However, there are advantages when using S-SEBI, such as the need of only one surface variable input (air temperature). In this case, the choice of the algorithm depends on both the availability of surface data and the intended application. In relation to Amazonia, a region with a lack of surface observations, S-SEBI may be a suitable proposition. Nevertheless, such as pointed out for SEBAL, the ideal application of S-SEBI in the region should focus on the use of MODIS composites.

3.1.3. Surface energy balance system (SEBS)

SEBS [74] is a single-source model developed to estimate the atmospheric turbulent fluxes using RS data. In single-source models, which also include SEBAL (Section 3.1.1) and S-SEBI (Section 3.1.2), the general assumption made is that the radiometric surface temperature measured by a radiometer (orbital sensor) is equivalent to aerodynamic surface temperature [75]. As discussed in the previous sections, these models are based on the difference between

dry and wet limits to estimate ET on a pixel-by-pixel basis. Such limits usually follow these characteristics: (1) maximum (minimum) LST, and (2) low or no (high or maximum) ET [41].

To generate such estimates, SEBS requires three types of input datasets. The first dataset consists on α_s, LST, vegetal cover fraction, and leaf area index (LAI) which usually obtained from RS images combined with specific information of the study area [76, 77]. Additional data includes vapor pressure deficit, air temperature and humidity, as well as wind speed, obtained from surface-level stations or reanalysis data. The third dataset is related to the incoming solar and thermal infrared radiation fluxes, which can be obtained directly from the surface-level measurements or reanalysis data.

Estimates of R_n and G follow the same assumptions as SEBAL and S-SEBI, while the estimates of H and λE present differences. In SEBS, for the dry limit, λE is assumed as zero (λE_{dry}), due to the soil moisture limitation, meaning that H reaches its maximum value (H_{dry}). Considering the wet limit, ET occurs in the potential rate (λE_{wet}), and H reaches its maximum value (H_{wet}). After the calculation of H_{dry}, H_{wet} and H, based on Monin-Obukhov Similarity Theory [78], the relative evaporation and reference evaporation fractions (Λ_r and Λ_{ref}, respectively) are obtained from Eqs. (2) and (3).

$$\Lambda_r = 1 - \frac{H - H_{wet}}{H_{dry} - H_{wet}} \tag{2}$$

$$\Lambda_{ref} = \frac{\Lambda_r \lambda E_{wet}}{R_n - G} \tag{3}$$

By inverting Eq. (3), it is possible to determinate λE for all pixels of the image. It is worth mentioning that during the parametrization of the turbulent processes in the layer immediately above the vegetation is necessary to define the surface roughness length [79]. Most of the algorithms consider a fixed value for the surface roughness length, while SEBS proposed a new formulation to define such variable, which, according to Li et al. [43], is one important advantage of using SEBS, since H is estimated more accurately.

Several studies have shown the potential of SEBS in daily, monthly and annually estimates of ET on local and regional scales [80–83]. Among the studies presented above, we highlight the work developed by Jia et al. [80] to estimate ET in the delta of the Yellow river in China. The authors used MODIS composites of reflectance, LST, and LAI to obtain ET values for 14 different land-use types, achieving mean square errors of ~0.9–1.3 mm. Overall, studies show that the errors between SEBS estimates and in situ measurements range between ~8 and 15% [84, 85]. Summarizing, SEBS presents advantages when compared to other algorithms, such as the surface roughness length estimate and the possibility of using MODIS composites; however, it requires a large number of surface parameters, which in regions like the Amazon can be an important issue.

3.1.4. Evapotranspiration assessment from space (EVASPA)

EVASPA [17] is a model developed to estimate ET using RS data considering spatial and temporal scales relevant for hydrological studies. Important characteristics of this algorithm include: (1) possibility of integrating data from multi-sensors, (2) estimation of the uncertainties, and (3) production of ET maps for days when there are no RS images available. EVASPA is based on S-SEBI [16] (Section 3.1.2) and the triangle method [85], which are very similar

in general. The study of Gillies et al. [86] provides a review of the principles of the triangle method to estimate ET.

EVASPA model is focused on generate ET estimates on the kilometric scale using MODIS sensor data from both Terra and Aqua satellites. However, the algorithm enables the generation of estimates using higher spatial resolution sensors, such as TM/LANDSAT 5 and ASTER/ Terra. In this regard, we highlight that this is a relatively recent model where equations for higher spatial resolution sensors are still not implemented. EVASPA estimates are generated using MODIS daily and eight- or 16-day data regarding α_s, LST, emissivity, LAI, and vegetation indices. The surface-level input data required consist in incoming solar and thermal infrared radiation. Numerical terrain information is also necessary and is usually obtained from the global digital elevation model GTOPO30 (http://edcdaac.usgs.gov/gtopo30/gtopo30.asp).

The model has several equations for each parameter necessary to estimate ET, such as R_n [65], G [87], and $\wedge$ [88]. Therefore, different estimates of ET are provided depending on the input data, enabling the evaluation of the uncertainties in the estimates of ET. Still, the model contains algorithms to interpolate ET estimates in days without orbital data or cloud cover [89]. Consequently, the model is an interesting option for applications in the Amazon, where it is difficult to obtain cloud free data in the region. Finally, it is worth mentioning the possibility of comparing EVASPA estimates with MODIS global ET product (MOD16) [90], which will be discussed in sequence. EVASPA generates as outputs graphics of accumulated monthly and annual ET, difference maps, and dispersion diagrams.

Initially, EVASPA validation was performed using in situ data acquired from a site located in southern France between 2009 and 2011 [17]. Mean square error corresponded to 0.78 mm, while R^2 was 0.76. It is noteworthy that both the characteristics of the model (i.e. reduced surface data required and the possibility of estimates for days without RS images available) and initial validation results are promising, therefore EVASPA presents a considerable potential for application in the Amazon region.

3.2. Models to estimate CO_2 fluxes

The eddy covariance system is the most common way to evaluate the carbon balance over terrestrial ecosystems [91]. However, estimates obtained from such system represent only fluxes at the tower scale, which ranges from hundreds of meters to a few kilometers. Therefore, many studies have been conducted aiming to understand the processes involving the carbon gained from ecosystems through photosynthesis and the carbon loss through respiration using RS data and modeling [53].

Most of the models are based on a radiation use efficiency (RUE) approach, although there are other empirical approaches. The concept of RUE was proposed by Monteith [92] and later became the basis for the use of RS to quantify the vegetation productivity. The algorithms are based on the relationship between RUE, absorbed photosynthetically active radiation (APAR), fraction of absorbed photosynthetically active radiation (fAPAR), and additional environmental variables that may limit photosynthesis [93]. Major difficulties in estimating RUE at large areas include dependency of environmental variables and the vegetation characteristics, as well as issues to estimating APAR (i.e. dependency of atmosphere dynamics) [94]. The primary outputs of these models are related to gross primary productivity (GPP), net

primary productivity (NPP), ecosystem respiration (R_{eco}), and net ecosystem carbon exchange (NEE). **Figure 2** [25] illustrates GPP estimates in the Amazon region using MODIS images.

3.2.1. Carnegie-Ames-Stanford approach (CASA)

CASA [95] is a model based on the processes of carbon assimilation and respiration to estimate NPP using satellite observations. The model incorporates assumptions of most biogeochemical algorithms, that is, CO_2 fluxes are controlled by ecosystem properties and driven by climate variability. The CASA formulation is based on the concept of vegetation greenness [96, 97]. Vegetation greenness level can be estimated from vegetation indices derived from RS, e.g. NDVI, given the good correlation between these indices with different biophysical parameters of the vegetation (i.e. fAPAR, LAI) [98].

CASA estimates NPP from RUE [92]. Thus, plant biomass production is estimated as a product of incoming solar radiation (K↓), fAPAR, and a term of radiation use efficiency (ε) ($\varepsilon = 0.389$ g C m^{-2} MJ^{-1}), which is multiplied by scale factors (f) of air temperature (T_{air}) and soil moisture (w), according to Eq. (4):
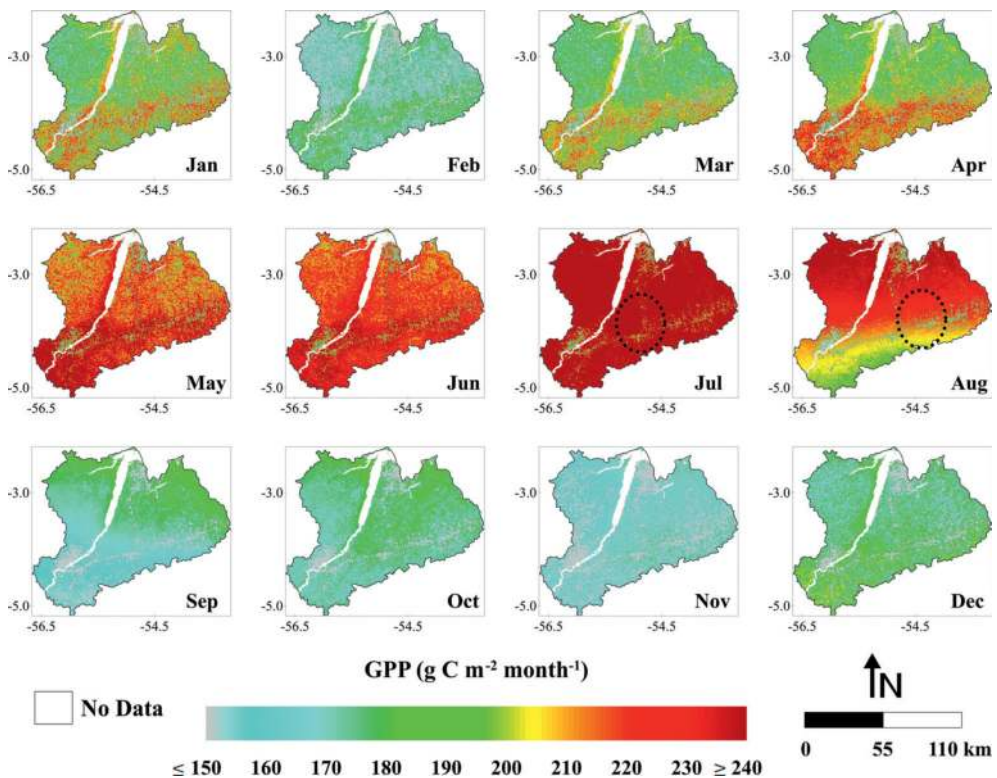

Figure 2. Obtained from the study of De Oliveira et al. [25]. Monthly averages of gross primary production (GPP) (g C m^{-2} $month^{-1}$), between the years 2001 and 2006, in the eastern flank of the Amazon region, using MODIS images. The black dashed circles show the spatial pattern of deforestation in the Amazon, known as the fish bone.

$$NPP = K{\downarrow}fAPAR\varepsilon f(T_{air})f(w) \tag{4}$$

As noted, air temperature and soil moisture are used to reduce the RUE from the maximum value. CASA requires surface measurements related to solar radiation, air temperature and precipitation as input data. The estimates generated from the model are usually well correlated with NPP obtained from the regional scale field observations; however, when compared to specific ecosystems (i.e. agricultural crops, forests and pastures) the correlations are low [99]. According to Yu et al. [100], this occurs because maximum RUE from CASA (ε = 0.389 g C m^{-2} MJ^{-1}) is not comparable to the RUE from diverse biomes.

3.2.2. Parametric production efficiency model (C-Fix)

C-Fix [18] is a model based on Monteith [92] and developed to quantify carbon fluxes on local, regional and global scales [101, 102]. Similar to CASA (Section 3.2.1), the key-element of C-Fix is that the biophysical state of the vegetation cover can be inferred from RS data. Therefore, C-Fix is basically derived from three steps: (1) mapping the vigor of the vegetation using NDVI estimated from orbital sensors, (2) estimation of fAPAR based on the relationship proposed by Myneni and Williams [103], and (3) inclusion of air temperature and incoming solar radiation measurements.

C-Fix provides the estimation of GPP, NPP, and net ecosystem productivity (NEP) according to the following equations:

$$GPP = f(T_{air})f(CO_{2,fert})\varepsilon fAPARcK{\downarrow} \tag{5}$$

$$NPP = GPP(1 - R_{a}) \tag{6}$$

$$NEP = NPP - R_{h} \tag{7}$$

In Eqs. (5)–(7), $f(T_{air})$ is a normalized factor of air temperature, $f(CO_{2,fert})$ is a normalized factor of CO_2 fertilization, ε is the term of radiation use efficiency (ε = 1.10 g C m^{-2} MJ^{-1}), c is the climatic efficiency (c = 0.48) [104], R_a is the autotropic respiration, and R_h is the heterotrophic respiration. Variables R_a and R_h are obtained from the algorithms proposed by Veroustraete et al. [105]. Maximum RUE in C-Fix is constant (ε = 1.10 g C m^{-2} MJ^{-1}), reduced by the normalizing factors of air temperature and fertilization by CO_2 dependency. Meteorological input data for the model are incoming solar radiation and air temperature.

Regarding C-Fix validation, studies indicate a reasonable correlation between fluxes estimated from the model and eddy covariance measurements (R^2~0.75) [18]. Recent upgrades in C-Fix, such as the insertion of hydric limitation functions have provided an improvement in the model performance when compared to field measurements [106]. However, there is a lack of studies to precisely evaluate the main sources of uncertainties in the model.

Studies conducted in Europe, using orbital data derived from AVHRR/NOAA and VEGETATION/ SPOT 4 [18, 107], show that the model provided a solid basis for estimating the temporal and

spatial distribution of the main components of the carbon budget in forest ecosystems on a regional scale. Such results, combined with the performance assessment and the requirement of few in situ information, show the potential of applying C-Fix in Amazonia.

3.2.3. Vegetation photosynthesis model (VPM)

VPM [108] was developed to estimate GPP in forest areas using vegetation indices obtained from optical sensors. During the last three decades, NDVI time series have been used in modeling GPP and NPP [109]; however, NDVI presents limitations, such as the sensitivity to atmospheric aerosols [110]. The inclusion of spectral bands located in the blue and short wave infrared regions in sensors such as the VEGETATION/SPOT 4 and MODIS/Terra and Aqua enabled the estimation of different vegetation indices that reduced some of the limitations and uncertainties imposed when merely using NDVI. In view of that, estimates generated from VPM consider EVI [111] and the land surface water index (LSWI) [112].

VPM is also based on an RUE approach, however it presents a key difference which is assuming that forest canopy is composed of photosynthetically active vegetation (PAV) (i.e. chloroplasts) and non-photosynthetically vegetation (NPV) (i.e. senescent leaves and branches) [97]. GPP estimated using VPM is obtained from the following equation:

$$GPP \ = \ \varepsilon fAPAR_{PAV} IPAR \qquad (8)$$

In Eq. (8), $fAPAR_{PAV}$ is the fraction of photosynthetically active radiation absorbed by PAV, and IPAR represents the incoming photosynthetically active radiation. $fAPAR_{PAV}$ is estimated as a linear function of EVI [108]. The contribution of fAPAR in $fAPAR_{PAV}$ and $fAPAR_{NPV}$ is important, since the presence of NPV significantly affects fAPAR at the canopy scale. For example, in forests with LAI < 3.0, NPV increased fAPAR by ~10–40% [113]. Also, it is important to point out that only $fAPAR_{PAV}$ is used in photosynthesis. Therefore, it is evident that this partition is a critical issue when modeling GPP or NPP in forests, considering $fAPAR_{PAV}$ may substantially increase the estimates. However, most of the CO_2 fluxes algorithms do not incorporate this assumption.

Another highlight of VPM is that the term ε is not constant, as opposed to CASA and C-Fix, varying according to the vegetation. ε parametrization in distinct forest formations is given by NEE and IPAR measurements obtained from flux towers located in specific sites. Research was conducted to define this variable in the boreal forest ($\varepsilon = 2.21$ g C m^{-2} MJ^{-1}) [108], and also in tropical rainforest ($\varepsilon = 2.48$ g C m^{-2} MJ^{-1}) [114]. Functions of air temperature, phenology, and water content of leaves (estimated from LSWI) are used to reduce the scale of ε. Required surface information of VPM are air temperature, NEE and IPAR.

Regarding the validation of VPM, Liu et al. [115] obtained R^2~0.88 when comparing the model outputs with surface measurements, while Jiang et al. [116] found relative errors of ~59%. According to Xiao et al. [108], the main sources of errors of VPM are related to the low sensitivity to PAR and air temperature, as well as the non-correction of the bidirectional effects on vegetation indices. VPM was applied to different forest ecosystems across the globe, among them, the Amazon rainforest [114]. The study conducted by Xiao et al. [114] used

VEGETATION/SPOT 4 and MODIS/Terra and Aqua (daily and 8-day composites) data to generate estimates of GPP over the FNT/K67 site in the state of Para, Brazil. The model estimates showed high NPP in the end of the dry season, which was consistent with the high ET and GPP measured by the micrometeorological tower.

VPM presents a high potential for the seasonal estimation of productivity in tropical forests. However, most of the studies using the model generated estimates only for the tower pixel and adjacent areas (i.e. 3x3 pixels) [114, 115]. Despite the possibility to retrieve GPP locally with a reasonable accuracy [108], the operationalization of VPM for regional analyzes requires modifications to the model, mainly related to the estimation of e for distinct forest formations and/or large areas.

3.2.4. Temperature and greenness rectangle model (TGR)

TGR [19] was developed to estimate the productivity of terrestrial ecosystems using MODIS/Terra and Aqua data. The model is based on studies conducted by Rahman et al. [117], in which a strong linear correlation between EVI and GPP in different forest formations was shown, and Sims et al. [118], which showed that LST can be used to infer the influence of water stress on GPP. Thus, TGR uses as inputs EVI and LST derived from MODIS and in situ IPAR measurements to estimate GPP on 16-day intervals. Three major aspects of TGR should be highlighted: (1) the algorithm strictly follows the RUE concept, (2) it has a low dependency of surface measurements, and (3) the overlapping of information in correlated explanatory variables is avoided.

Based on the proposition of Monteith [92], GPP in TGR model is estimated according to Eq. (9):

$$\text{GPP } = \ \varepsilon * \text{f(EVI, L, ST)IPAR} \tag{9}$$

The term ε^* refers to the amount of carbon fixed per unit of IPAR. It should be noted that this assumption is different from the traditional definition of RUE, which is the amount of carbon fixed per unit of APAR. In TGR, as well as in most of the vegetation productivity models, the term of radiation use efficiency is multiplied by a scale factor, aiming to reduce estimates under unfavorable conditions (i.e. high or low temperature and high vapor pressure deficit). For this purpose, EVI [119] and LST [108] are used. According to Yang et al. [19], it is inappropriate to simply multiply the effect of these two variables, considering that both are physically interdependent. Therefore, to define the f value from EVI and LST the algorithm proposes a methodology based on the least square method [19]. Studies indicate that IPAR may range from ~40 to 50% of the incoming solar radiation [120]. Thus, Yang et al. [19] suggest the use of in situ measurements of this variable in order to reduce the uncertainties.

In TGR, as for VPM (Section 3.2.3), the term RUE is not constant, allowing the calibration for different vegetation formulations. The study of Yang et al. [19] described values of this term for eight types of vegetation, including pasture, savanna, and mixed forest. This study also validated the model considering measurements obtained from 13 different experimental sites in the United States. Results showed that estimates from TGR agreed with tower flux measurements for almost all types of vegetation, with $R^2{\sim}0.67$–0.91. TGR allows to capture the GPP patterns over large areas, which is necessary for applications in the Amazon region.

In this context, we highlight that the use of IPAR data obtained directly from MODIS [121] would eliminate the need of in situ measurements, enhancing the potential of TGR for applications in Amazonia. According to Yang et al. [19], future studies will focus on validating TGR estimates over tropical forest areas.

3.3. Remote sensing global products

RS is the main tool for observing the state and processes of terrestrial surface and atmosphere [122]. LANDSAT, SPOT, NOAA, Terra and Aqua platforms have provided time series of data in different spatial and temporal resolutions, which are applied in a wide range of studies [123]. One application is related to global climate change, where RS data have been used as inputs in climate models to simulate climate dynamics and future projections [124]. Accordingly, it is notable an effort of the scientific community in generating RS derived standardized global products, specially related to the biophysical domain.

Currently, some of the most important global products based on satellite observations are derived from MODIS/Terra and Aqua sensors. MODIS was developed by the Goddard Space Flight Center (GSFC/NASA) and presents an imaging system composed by 36 spectral bands, from the visible to the thermal infrared regions. MODIS temporal resolution is daily for latitudes above 30° and 2 days for latitudes below 30° [125]. Surface products derived from MODIS are related to α_s [126], LST [127], vegetation indices [128], land-use [129] and other variables. More specifically, regarding energy and carbon fluxes, we highlight the ET (MOD16) [90], GPP and NPP (MOD17) [130] products.

3.3.1. MOD16

The MOD16 [90] product was developed to estimate global surface ET from MODIS/Terra and Aqua data and meteorological information obtained from the Global Modeling and Assimilation Office (GMAO). The algorithm is based on Penmann-Monteith equation [46]:

$$ET = \frac{\Delta(R_n - G) + \varrho_a c_p (e_s - e_a)/r_a}{\Delta + \gamma(1 + {}^{r_s}\!/_{r_a})} \tag{10}$$

In Eq. (10), Δ is the gradient of saturated vapor pressure to air temperature, R_n is the net radiation, G is the soil heat flux, ϱ_a is the air density, c_p is the specific heat of air at constant pressure, e_s and e_a are the saturated vapor pressure and actual vapor pressure, respectively, γ is the psychometric constant (0.066 kPa°C^{-1}), and r_s and r_a are the surface and aerodynamic resistance, respectively. MODIS input data in the algorithm include α_s, LAI, and land-use. Regarding the meteorological variables, solar radiation, air temperature, and water vapor pressure reanalysis data are used. Summarizing, MOD16 data are provided with spatial resolution of 500 m and 1 km and cover an area of ~109 millions of km^2. MOD16 provides potential and actual ET fluxes at 8 days, monthly and annual intervals.

MOD16 was initially validated using measurements from 46 different tower fluxes across the United States, obtaining R^2~0.65 [90]. It is possible to point out main two sources of uncertainties related to MOD16: (1) GMAO reanalysis data, mostly due to the low spatial resolution (~100 km) when compared to MOD16 (500 m and 1 km), and (2) LAI and land-use products,

which may present reasonable inaccuracies depending on the biome, which, consequently, will result in the incorrect determination of parameters to calculate plants transpiration [90]. Most studies using MOD16 are focused on Asia and Middle East, aiming to evaluate watersheds [131, 132] and different land-uses, especially in agricultural areas [133]. Validation performed on such studies agree with results found by Mu et al. [90].

Recent studies validated MOD16 in the Cerrado and Amazon biomes [45, 25]. Over Cerrado, the algorithm presented relative high correlation coefficients, ranging between ~0.78 and 0.81 [45]. Results obtained for the Amazon were less satisfactory. Validation performed using tower fluxes data located over forest and pasture areas showed R^2 values between ~0.32 and 0.76 [25]. It should be noted that simplifications in MOD16 algorithm regarding some parameters such as canopy conductance are defined as constant for a given biome (even in a heterogeneous one, such as the Amazon). This may be one of the reasons for low correlations between the estimated and observed data in the region. This is actually one of the main challenges of global algorithms, which need to be complex to accurately represent the physical processes on the surface, and simultaneously simple enough to be implemented globally [45]. Despite this, MOD16 was able to represent the spatial variability of ET in the Amazon. This is an important result and one interesting way to better evaluate the results of this model for the Amazon would be through the comparison between MOD16 outputs with more local estimates based on the models described in Sections 3.1.1–3.1.4.

3.3.2. MOD17

The MOD17 product [130] provides continuous estimates of GPP and NPP over the vegetated surface of the planet. As well as models described in Sections 3.2.1–3.2.4, the MOD17 algorithm is based on the RUE approach [92]. According to this approach, the productivity of vegetation under reasonable water and soil fertility conditions is linearly correlated with the amount of APAR. MOD17 is based on three basic relationships (Eqs. (11)–(13)) to estimate GPP and net photosynthesis (PS_{Net}), on eight-day and monthly intervals, and annual NPP.

$$GPP = \varepsilon\left(T_{air,min}\right)f(VPD)APAR \tag{11}$$

$$PS_{Net} = GPP - R_{lr} \tag{12}$$

$$NPP = \sum\left(PS_{Net}\right) - R_g - R_m \tag{13}$$

In the equations presented above, $f(T_{air,min})$ and $f(VPD)$ are scale factors associated, respectively, to minimum air temperature and vapor pressure deficit, R_{lr} is the maintenance respiration of leaves and thin roots, R_g is the growing respiration, and R_m represents the maintenance respiration of living cells in the woody tissue. It is worth mentioning that the algorithm defines distinct values for ε, depending on the vegetation. ε values are distinct for forest, savanna, pasture, and agricultural areas. $T_{air,min}$ and VPD values, as well as respiration values, are based on a lookup table composed of specific physiological parameters for each terrestrial biome [134]. MOD17 product is estimated from MODIS standard products (i.e. fAPAR and LAI) and reanalysis data (i.e. air temperature and solar radiation) from the National Center

for Environmental Prediction/National Center for Atmospheric Research (NCEP/NCAR). MOD17 outputs (GPP, PS_{Net} (eight-day and monthly), and NPP (annual)), as well as MOD16 outputs, are provided with 500 m and 1 km spatial resolution.

Validation studies comparing MOD17 estimates with flux tower measurements found relative errors between ~24 and 70%, and correlation coefficients ranging between ~0.26 and 0.88 [135–137]. Generally, GPP and NPP derived from MOD17 follow the expected seasonal patterns according to the land-use and climate; however, values tend to be overestimated over low productivity sites (i.e. croplands), and underestimated over high productivity sites (i.e. forests). The main sources of errors in MOD17 are associated with the MODIS fAPAR product and reanalysis data [138].

MOD17 product has been validated over different regions [137, 139, 140]. Regarding the Amazon, an important area in the global carbon cycle, we highlight the study recently developed by De Oliveira et al. [25] in Para state, eastern Brazilian Amazonia. The mean relative error found for MOD17 GPP was about 13% of the field measurements (LBA flux towers). An underestimation was observed for primary and secondary forests (−4.1 and − 3.6 g C m^{-2}, respectively) and an overestimation for pasture (2.2 g C m^{-2}). According to the authors, the MOD17 product was able to provide reliable information about the spatial and temporal variability of GPP in the eastern flank of Amazonia.

4. Concluding remarks

Micrometeorological studies in Amazonian ecosystems have limited spatial and temporal coverage, and therefore RS becomes a tool to enhance the comprehension of surface processes in the region. Models to estimate energy and carbon balance components from orbital data differ according to the input data, parametrizations and accuracy of the results. The algorithms to estimate energy fluxes use as inputs images from visible and infrared (near and thermal) spectral regions and are based on empirical and physical methods. In situ measurements are typically related to air temperature and wind speed, and most uncertainties are concentrated in the estimation of H and ET (when obtained as a residual term of the energy budget). On the other hand, CO_2 fluxes models need data from the visible and near infrared spectral regions and are based on the RUE concept. Main challenges of such models consist in the estimation of RUE for different ecosystems, as well as to obtain surface solar radiation data with a reasonable spatial resolution.

Regarding the use of such models in the Amazon region, some difficulties emerge: (1) obtaining cloud free orbital data, and (2) availability of field observations. Therefore, the choice of the algorithm must consider the possibility of using daily composites, and minimal need of in situ data. Other issues, such as the complexity and operability of the models may be considered. It is then possible to point out algorithms that present greater potential of application in the region and/or where efforts for implementation should focus. Regarding energy balance, two models stand out: SEBAL [47], due to the reduced need for field measurements and because the model was previously validated in the region and showed good results, and EVASPA [17], due to the operability and possibility of generating estimates during days when there are no orbital data available. In relation to the carbon models, it is suggested the use of

VPM [108], once the model was applied to distinct forest ecosystems (including the Amazon) showing good results, and TGR [19], due to the fact that the model is based on MODIS composites and has a low dependence of field data.

Regarding the use of global RS products in the Amazon, it is important to emphasize that such products usually enable the analysis of spatial patterns of surface parameters; however, they present inaccuracies when referring to the magnitude of the estimates. A noteworthy aspect is that studies conducted in tropical regions, among them the Amazon, have proposed methodologies based on integrating satellite images and reanalysis climate data in hydrological and ecosystem models based on local measurements [2, 22, 23, 45, 141, 142]. Although there are difficulties, for example those related to representing the ecophysiological processes from leaf to canopy scale, such approaches constitute promising opportunities for future research.

The use of models based on satellite images presents an important role in understanding the spatial and temporal patterns of biophysical surface parameters in a region where most of the information is local. Data generated from such algorithms may be used as inputs in earth system surface models allowing, among others, to evaluate the impact, both in regional and global scales, caused by land-use and land-cover changes.

Acknowledgements

Author details

Gabriel de Oliveira[1,2]*, Nathaniel A. Brunsell[1], Elisabete C. Moraes[2], Yosio E. Shimabukuro[2], Guilherme A. V. Mataveli[3], Thiago V. dos Santos[4], Celso von Randow[2] and Luiz E. O. C. Aragao[2,5]

*Address all correspondence to: gabrieloliveira@ku.edu

1 Department of Geography and Atmospheric Science, University of Kansas, Lawrence, KS, USA

2 National Institute for Space Research, Sao Paulo, Brazil

3 Department of Geography, University of Sao Paulo, Sao Paulo, Brazil

4 Department of Climate and Space Sciences and Engineering, University of Michigan, Ann Arbor, MI, USA

5 College of Life and Environmental Sciences, University of Exeter, Exeter, UK

References

[1] Davidson EA, Araújo AC, Artaxo Netto PE, Balch JK, Brown IF, Bustamante MM, et al. The Amazon basin in transition. Nature. 2012;**481**(7381):321-328. DOI: 10.1038/nature10717

[2] Ahlstrom A, Canadell JP, Schurgers G, Wu M, Berry JA, Guan K, et al. Hydrologic resilience and Amazon productivity. Nature Communications. 2017;**8**:1-9. DOI: 10.1038/s41467-017-00306-z

[3] Swann AL, Fung IY, Chiang JC. Mid-latitude afforestation shifts general circulation and tropical precipitation. Proceedings of the National Academy of Sciences. 2012;**109**(3):1196-1206. DOI: 10.1073/pnas.1116706108

[4] Zanchi FB, Waterloo MJ, Tapia AP, Alvarado Barrientos MS, Bolson MA, Luizão FJ, et al. Water balance, nutrient and carbon export from a heath forest catchment in Central Amazonia, Brazi. Hydrological Processes. 2015;**29**(17):3633-3648. DOI: 10.1002/hyp.10458

[5] Von Randow C, Manzi AO, Kruijt B, Oliveira PJ, Zanchi FB, Silva RL, et al. Comparative measurements and seasonal variations in energy and carbon exchange over forest and pasture in south West Amazonia. Theoretical and Applied Climatology. 2004;**78**(1-3):5-26. DOI: 10.1007/s00704-004-0041-z

[6] Querino CAS, Moura MAL, Lyra RFF, Mariano GL. Evaluation and comparison of global solar radiation and albedo with zenith angle in the Amazon region. Brazilian Journal of Meteorology. 2006;**21**(3):42-49

[7] Stark SC, Breshears DD, Garcia ES, Law DJ, Minor DM, Saleska SR, et al. Toward accounting for ecoclimate teleconnections: Intra-and inter-continental consequences of altered energy balance after vegetation change. Landscape Ecology. 2016;**31**(1):181-194. DOI: 10.1007/s10980-015-0282-5

[8] Houborg R, Soegaard H, Emmerich W, Moran S. Inferences of all sky solar irradiance using Terra and Aqua MODIS satellite data. International Journal of Remote Sensing. 2007;**28**(20):4509-4535. DOI: 10.1080/01431160701241902

[9] El-Masri B, Jain AK, Barman R, Meiyappan P, Song Y, Liang M. Carbon dynamics in the Amazonian basin: Integration of eddy covariance and ecophysiological data with a land surface model. Agricultural and Forest Meteorology. 2013;**182-183**(15):156-167. DOI: 10.1016/j.agrformet.2013.03.011

[10] Malhi Y, Pegoraro E, Nobre AD, Pereira MGP, Grace J, Culf AD, et al. Energy and water dynamics of a central Amazonian rain forest. Journal of Geophysical Research. 2002;**107**(D2070):1-17. DOI: 10.1029/2001JD000623

[11] Zeri M, Sá LD, Manzi AO, Araújo AC, Aguiar RG, Von Randow C, et al. Variability of carbon and water fluxes following climate extremes over a tropical forest in southwestern Amazonia. PLoS One. 2014;**9**(2):e88130. DOI: 10.1371/journal.pone.0088130

[12] Papadavid G, Hadjimitsis D. Adaptation of SEBAL for estimating groundnuts evapo-transpiration, in Cyprus. South-Eastern European Journal of Earth Observation and Geomatics. 2012;**1**(2):59-70

[13] Wang S, Pan M, Mu Q, Shi X, Mao J, Brümmer C, et al. Comparing evapotranspiration from Eddy covariance measurements, water budgets, remote sensing, and land surface models over Canada. Journal of Hydrometeorology. 2015;**16**(4):1540-1560. DOI: 10.1175/JHM-D-14-0189.1

[14] Bhattarai N, Dougherty M, Marzen LJ, Kalin L. Validation of evaporation estimates from a modified surface energy balance algorithm for land (SEBAL) model in the South-Eastern United States. Remote Sensing Letters. 2012;**3**(6):511-519. DOI: 10.1080/01431161.2011.632655

[15] Du J, Song K, Wang Z, Zhang B, Liu D. Evapotranspiration estimation based on MODIS products and surface energy balance algorithms for land (SEBAL) model in Sanjiang Plain, Northeast China. Chinese Geographical Science. 2013;**23**(1):73-91

[16] Roerink GJ, Su Z, Menenti M. S-SEBI: A simple remote sensing algorithm to estimate the surface energy balance. Physics and Chemistry of the Earth Part B. 2000;**25**(2):147-157. DOI: 10.1016/S1464-1909(99)00128-8

[17] Gallego-Elvira B, Olioso A, Mira M, Reyes-Castillo S, Boulet G, Marloie O, et al. EVASPA (EVapotranspiration assessment from SPAce) tool: An overview. Procedia Environmental Sciences. 2013;**19**:303-310. DOI: 10.1016/j.proenv.2013.06.035

[18] Veroustraete F, Sabbe H, Herman E. Estimation of carbon mass fluxes over Europe using the C-Fixmodel and Euroflux data. Remote Sensing of Environment. 2002;**83**(3):376-399. DOI: 10.1016/S0034-4257(02)00043-3

[19] Yang Y, Shang S, Guan H, Jiang L. A novel algorithm to assess gross primary production for terrestrial ecosystems from MODIS imagery. Journal of Geophysical Research. 2013a;**118**(2):590-605. DOI: 10.1002/jgrg.20056

[20] Potter CS, Klooster S, Huete A, Genovese V, Bustamante M, Ferreira LG, et al. Terrestrial carbon sinks in the Brazilian Amazon and Cerrado region predicted from MODIS satellite data and ecosystem modeling. Biogeosciences Discussions. 2009;**6**(6):947-969. DOI: 10.5194/bg-6-937-2009

[21] De Oliveira G, Moraes EC. Validation of net radiation obtained from MODIS/Terra data in Amazonia with LBA surface measurements. Acta Amazonica. 2013;**43**(3):353-364

[22] De Oliveira G, Brunsell NA, Moraes EC, Bertani G, Dos Santos TV, Shimabukuro YE, et al. Use of MODIS sensor images combined with reanalysis products to retrieve net radiation in Amazonia. Sensors. 2016;**16**(7):1-28. DOI: 10.3390/s16070956

[23] Khand K, Numata I, Kjaersgaard J, Vourlitis GL. Dry season evapotranspiration dynamics over human-impacted landscapes in the southern Amazon using the Landsat-based METRIC model. Remote Sensing. 2017;**9**(7):1-20. DOI: 10.3390/rs9070706

[24] Numata I, Khand K, Kjaersgaard J, Cochrane MA, Silva SS. Evaluation of Landsat-based METRIC modeling to provide high-spatial resolution evapotranspiration estimates for Amazonian forests. Remote Sensing. 2017;**9**(46):1-19. DOI: 10.3390/rs9010046

[25] De Oliveira G, Brunsell NA, Moraes EC, Shimabukuro YE, Bertani G, Dos Santos TV, et al. Evaluation of MODIS-based estimates of water-use efficiency in Amazonia. International Journal of Remote Sensing. 2017;**38**(19):5291-5309. DOI: 10.1080/01431161.2017.1339924

[26] Shuttleworth WJ, Gash JHB, Lloyd CR, Moore CJ, Roberts J, Molion LCB, et al. Amazonian evaporation. Brazilian Journal of Meteorology. 1987;**2**(1):179-191

[27] Garstang M, Ulanski S, Greco S, Scala J, Swap R, Fitzjarrald D, et al. The Amazon boundary layer experiment (ABLE 2B): A meteorological perspective. Bulletin of the American Meteorological Society. 1990;**71**(1):19-32. DOI: 10.1175/1520-0477(1990)071<0019:TABLEA>2.0.CO;2

[28] Gash JHC, Nobre CA. Climatic effects of Amazonian deforestation: Some results from ABRACOS. Bulletin of the American Meteorological Society. 1997;**78**(5):823-830. DOI: 10.1175/1520-0477(1997)078<0823:CEOADS>2.0.CO;2

[29] Martin ST, Artaxo P, Machado LAT, Manzi AO, Souza RAF, Schumacher C, et al. Introduction: Observations and modeling of the Green Ocean Amazon (GoAmazon2014/5). Atmospheric Chemistry and Physics. 2015;**16**(8):4785-4797. DOI: 10.5194/acp-16-4785-2016

[30] Artaxo PE. Break down boundaries in climate research. Nature. 2012;**481**(239). DOI: 10.1038/481239a

[31] Gonçalves LGG, Borak JS, Costa MN, Saleska SR, Baker I, Restrepo-Coupe N, et al. Overview of the large-scale biosphere atmosphere experiment in Amazônia data model Intercomparison project (LBA DMIP). Agricultural and Forest Meteorology. 2013;**182-183**(15):111-127. DOI: 10.1016/j.agrformet.2013.04.030

[32] Culf AD, Fisch G, Hodnett MG. The albedo of Amazonian forest and ranchland. Journal of Climate. 1995;**8**(6):1544-1554. DOI: 10.1175/1520-0442(1995)008<1544:TAOAFA>2.0.CO;2

[33] Leitão MMVBR, Santos JM, Oliveira GM. Estimatin of albedo in three ecosystems of the Amazon forest. Brazilian Journal of Agricultural and Environmental Engineering. 2002;**6**(2):256-261. DOI: 10.1590/S1415-43662002000200013

[34] Alves FSM, Fisch G, Vendrame IF. Microclimate and hidrology modifications due to the deforestation in Amazonia: A case study in Rondonia state (RO), Brazil. Acta Amazonica. 1999;**29**(3):395-409. DOI: 10.1590/1809-43921999293409

[35] Rocha HR, Goulden ML, Miller SD, Menton MC, Pinto LDVO, Freitas HC, et al. Seasonality of water and heat fluxes over a tropical forest in eastern Amazonia. Ecological Applications. 2004;**14**(sp4):522-532. DOI: 10.1890/02-6001

[36] Sakai RK, Fitzjarrald DR, Moraes OLL, Staebler RM, Acevedo OC, Czikowsky MJ, et al. Land-use change effects on local energy, water, and carbon balances in an Amazonian agricultural field. Global Change Biology. 2004;**10**(5):895-907. DOI: 10.1111/j.1529-8817.2003.00773.x

[37] Hutyra LR, Munger JW, Saleska SR, Gottlieb E, Daube BC, Dunn AL, et al. Seasonal controls on the exchange of carbon and water in an Amazonian rain forest. Journal of Geophysical Research. 2007;**112**(G3):1-16. DOI: 10.1029/2006JG000365

[38] Negrón-Juárez RI, Goulden ML, Myneni RB, Fu R, Bernardes S, Gao H. An empirical approach to retrieve monthly evapotranspiration over Amazonia. International Journal of Remote Sensing. 2008;**2**(24):7045-7063. DOI: 10.1080/01431160802226026

[39] Gloor M, Gatti L, Brienen RJW, Feldpausch T, Phillips O, Miller J, et al. The carbon balance of South America: Status, decadal trends and main determinants. Biogeosciences. 2012;**9**(12):5407-5430. DOI: 10.5194/bg-9-5407-2012

[40] Raschke E, Preuss HJ. The determination of the solar radiation budget at the earth's surface from satellite measurement. Meteorologic Rundschau. 1979;**32**(1):18-28

[41] Gowda PH, Chavez JL, Colaizzi PD, Evett SR, Howell TA, Tolk JA. ET mapping for agricultural water management: Present status and challenges. Irrigation Science. 2008;**26**(3):223-237. DOI: 10.1007/s00271-007-0088-6

[42] Yang Y, Shang S, Jiang L. Remote sensing temporal and spatial patterns of evapotranspiration and the responses to water management in a large irrigation district of North China. Agricultural and Forest Meteorology. 2012;**164**(15):112-122. DOI: 10.1016/j.agrformet.2012.05.011

[43] Li ZL, Tang R, Wan Z, Bi Y, Zhou C, Tang B, et al. A review of current methodologies for regional evapotranspiration estimation from remotely sensed data. Sensors. 2009;**9**(5):3801-3853. DOI: 10.3390/s90503801

[44] French AN, Hunsaker DJ, Thorp KR. Remote sensing of evapotranspiration over cotton using the TSEB and METRIC energy balance models. Remote Sensing of Environment. 2015;**158**(1):281-294. DOI: 10.1016/j.rse.2014.11.003

[45] Ruhoff AL, Paz AR, Aragao LEOC, Collischonn W, Mu Q, Malhi YS, et al. Assessment of the MODIS global evapotranspiration algorithm using eddy covariance measurements and hydrological modelling in the Rio Grande basin. Hydrological Sciences Journal. 2013;**58**(8):1658-1676. DOI: 10.1080/02626667.2013.837578

[46] Monteith JL. Evaporation and environment. In: Symposium of the Society of Experimental Biology; 1965. pp. 205-224

[47] Bastiaanssen WGM, Menenti M, Feddes RA, Holtslag AAM. A remote sensing surface energy balance algorithm for land (SEBAL): Formulation. Journal of Hydrology. 1998;**212-213**(1-4):198-212. DOI: 10.1016/S0022-1694(98)00253-4

[48] Liang S. Narrowband to broadband conversions of land surface albedo I algorithms. Remote Sensing of Environment. 2001;**76**(2):213-238. DOI: 10.1016/S0034-4257(00)00205-4

[49] Bastiaanssen WGM. SEBAL-based sensible and latent heat fluxes in the irrigated Gediz Basin, Turkey. Journal of Hydrology. 2000;**229**(1-2):87-100. DOI: 10.1016/S0022-1694(99)00202-4

[50] Allen R, Irmak A, Trezza R, Hendrickx JMH, Bastiaanssen W, Kjaersgaard J. Satellite-based ET estimation in agriculture using SEBAL and METRIC. Hydrological Processes. 2011;**25**(26):4011-4027. DOI: 10.1002/hyp.8408

[51] Kjaersgaard J, Allen RG, Irmak A. Improved methods for estimating monthly and growing season ET using METRIC applied to moderate resolution satellite imagery. Hydrological Processes. 2011;**25**(26):4028-4036. DOI: 10.1002/hyp.8394

[52] Paiva CM, França GB, Liu WTH, Rotunno Filho OC. A comparison of experimental energy balance components data and SEBAL model results in Dourados, Brazil. International Journal of Remote Sensing. 2011;**32**(6):1731-1745. DOI: 10.1080/01431161003623425

[53] Tang R, Li ZL, Chen KS, Jia Y, Li C, Sun X. Spatial-scale effect on the SEBAL model for evapotranspiration estimation using remote sensing data. Agricultural and Forest Meteorology. 2013;**147-175**(15):28-42. DOI: 10.1016/j.agrformet.2013.01.008

[54] Yang JY, Mei XR, Huo ZG, Yan CR, Hui JU, Zhao FH, Qin LIU. Water consumption in summer maize and winter wheat cropping system based on SEBAL model in Huang-Huai-Hai plain, China. Journal of Integrative Agriculture. 2015;**14**(10):2065-2076. DOI: 10.1016/S2095-3119(14)60951-5

[55] Senay GB, Budde M, Verdin JP, Melesse AM. A coupled remote sensing and simplified surface energy balance approach to estimate actual evapotranspiration from irrigated fields. Sensors. 2007;**7**(2):979-1000. DOI: 10.3390/s7060979

[56] Schuurmans JM, Van Geer FC, Bierkens MPF. Remotely sensed latent heat fluxes for model error diagnosis: A case study. Hydrology and Earth System Sciences. 2011;**15**:759-769. DOI: 10.5194/hess-15-759-2011

[57] Bastiaanssen WGW, Pelgrum H, Wang J, Ma Y, Moreno J, Roerink GJ, Van Der Wal T. A remote sensing surface energy balance algorithm for land (SEBAL): Validation. Journal of Hydrology. 1998;**212-213**:213-229. DOI: 10.1016/S0022-1694(98)00254-6

[58] Hemakumara HM, Chandrapala L, Moene AF. Evapotranspiration fluxes over mixed vegetation areas measured from large aperture scintillometer. Agricultural Water Management. 2003;**58**(2):109-122. DOI: 10.1016/S0378-3774(02)00131-2

[59] Kimura RLB, Fan J, Takayama N, Hinokidani O. Evapotranspiration estimation over the river basin of the loess plateau of China based on remote sensing. Journal of Arid Environments. 2007;**68**(1):53-65. DOI: 10.1016/j.jaridenv.2006.03.029

[60] Liberato AM, Silva BB, Cardoso FL. Use of techniques of remotes sensing in the estimation of net radiation in Rondonia. Pesquisa e Criacao. 2011;**10**(2):153-164

[61] Santos CAC, Nascimento RL, Rao TVR, Manzi AO. Net radiation estimation under pasture and forest in Rondônia, Brazil, with TM Landsat 5 images. Atmosfera. 2011; **24**(4):435-446

[62] Ferreira P, Sousa AM, Vitorino MI, Souza EB, Souza PJOP. Estimate of evapotranspiration in the eastern Amazon using SEBAL. Brazilian Journal of Agricultural Sciences. 2013;**56**(1):33-39. DOI: 10.4322/rca.2013.001

[63] Justice CO, Townshend JRG, Vermote EF, Masuoka E, Wolfe RE, Saleous N, et al. An overview of MODIS land data processing and product status. Remote Sensing of Environment. 2002;**83**(1-2):3-15. DOI: 10.1016/S0034-4257(02)00084-6

[64] Ouaidrari H, Gowart SN, Czajkowski KP, Sobrino JA, Vermote E. Land surface temperature estimation from AVHRR thermal infrared measurements: An assessment for the AVHRR land pathfinder II data set. Remote Sensing of Environment. 2002;**81**(1):114-128. DOI: 10.1016/S0034-4257(01)00338-8

[65] Sobrino JA, Gomez M, Jimenez-Munoz JC, Olioso A. Application of a simple algorithm to estimate daily evapotranspiration from NOAA-AVHRR images for the Iberian peninsula. Remote Sensing of Environment. 2007;**110**(2):139-148. DOI: 10.1016/j.rse.2007.02.017

[66] Bhattarai N, Shaw SB, Quackenbush LJ, Im J, Niraula R. Evaluating five remote sensing based single-source surface energy balance models for estimating daily evapotranspiration in a humid subtropical climate. International Journal of Applied Earth Observation and Geoinformation. 2016;**49**:75-86. DOI: 10.1016/j.jag.2016.01.010

[67] Sobrino JA, Gomez M, Jimenez-Munoz JC, Olioso A, Chehbouni G. A simple algorithm to estimate evapotranspiration from DAIS data: Application to the DAISEX campaigns. Journal of Hydrology. 2005;**315**(1-4):117-125. DOI: 10.1016/j.jhydrol.2005.03.027

[68] Van Der Tol C. Validation of remote sensing of bare soil ground heat flux. Remote Sensing of Environment. 2012;**121**:275-286. DOI: 10.1016/j.rse.2012.02.009

[69] Fan L, Liu S, Bernhofer C, Liu H, Berger FH. Regional land surface energy fluxes by satellite remote sensing in the upper Xilin River watershed (Inner Mongolia, China). Theoretical and Applied Climatology. 2007;**88**(3-4):231-245. DOI: 10.1007/s00704-006-0241-9

[70] Brunner P, Li HT, Kinzelbach W, Li WP, Dong XG. Extracting phreatic evaporation from remotely sensed maps of evapotranspiration. Water Resources Research. 2008;**44**(8):1-12. DOI: 10.1029/2007WR006063

[71] Galleguillos M, Jacob F, Prévot L, Lagacherie P, Liang S. Mapping daily evapotranspiration over a Mediterranean vineyard watershed. IEEE Geoscience and Remote Sensing Letters. 2011;**8**(1):168-172. DOI: 10.1109/LGRS.2010.2055230

[72] Santos CAC, Silva BB. Obtenção dos fluxos de energia à superfície utilizando o algoritmo S-SEBI. Revista Brasileira de Meteorologia. 2010;**25**(3):365-374

[73] Lazarim CG. Estimation of Evapotranspiration and Surface Temperature Trhough Images of Satellite AVHRR/NOAA for Agricultural Monitoring [Dissertation]. Campinas:

Universidade Estadual de Campinas; 2013. p. 112. Available from: http://bdtd.ibict.br/vufind/Record/CAMP_eb1e7f06dbb0101827a66f93f97cbc2c/Details

[74] Su Z. The surface energy balance system (SEBS) for estimation of turbulent fluxes. Hydrology and Earth System Sciences. 2002;**6**:85-100. DOI: 10.5194/hess-6-85-2002

[75] Timmermans W, Kustas WP, Anderson MC, French AN. An intercomparison of the surface energy balance algorithms for land (SEBAL) and the two-source energy balance (TSEB) modeling schemes. Remote Sensing of Environment. 2007;**108**(4):369-384. DOI: 10.1016/j.rse.2006.11.028

[76] Su Z, Pelgrum H, Menenti M. Aggregation effects of surface heterogeneity in land surface processes. Hydrology and Earth System Sciences. 1999;**3**:549-563. DOI: 10.5194/hess-3-549-1999

[77] Li ZL, Stoll MP, Zhang R, Jia L, Su Z. On the separate retrieval of soil and vegetation temperatures from ATSR data. Science in China Series D: Earth Sciences. 2000;**30**:27-38. DOI: 10.1007/BF02879653

[78] Monin AS, Obukhov AM. Basic laws of turbulent mixing in the atmosphere near the ground. Trudy Geofizicheskogo Instituta, Akademiya Nauk SSSR. 1954;**24**:163-187

[79] Takagi K, Miyata A, Harazono Y, Ota N, Komine M, Yoshimoto M. An alternative approach to determining zero-plane displacement, and its application to a lotus paddy field. Agricultural and Forest Meteorology. 2003;**115**(3-4):173-181. DOI: 10.1016/S0168-1923(02)00209-5

[80] Jia L, Xi G, Liu S, Huang C, Yan Y, Liu G. Regional estimation of daily to annual regional evapotranspiration with MODIS data in the Yellow River Delta wetland. Hydrology and Earth System Sciences. 2009;**13**:1775-1787. DOI: 10.5194/hess-13-1775-2009

[81] Elhag M, Psilovikos A, Manakos I, Perakis K. Application of the SEBS water balance model in estimating daily evapotranspiration and evaporative fraction from remote sensing data over the Nile delta. Water Resources Management. 2011;**25**(11):2731-2742. DOI: 10.1007/s11269-011-9835-9

[82] Ma W, Hafeez M, Ishikawa H, Ma Y. Evaluation of SEBS for estimation of actual evapotranspiration using ASTER satellite data for irrigation areas of Australia. Theoretical and Applied Climatology. 2013;**112**(3-4):609-616. DOI: 10.1007/s00704-012-0754-3

[83] Shoko C, Dube T, Sibanda M, Adelabu S. Applying the surface energy balance system (SEBS) remote sensing model to estimate spatial variations in evapotranspiration in southern Zimbabwe. Transactions of the Royal Society of South Africa. 2015;**70**(1):47-55. DOI: 10.1080/0035919X.2014.989933

[84] Su H, Mccabe MF, Wood EF, Su Z, Prueger JH. Modelling evapotranspiration during SMACEX: Comparing two approaches for local- and regional-scale prediction. Journal of Hydrometeorology. 2005;**6**:910-922. DOI: 10.1175/JHM466.1

[85] Moran M, Clarke T, Inoue Y, Vidal A. Estimating crop water deficit using relation between surface-air temperature and spectral vegetation index. Remote Sensing of Environment. 1994;**49**(3):246-263. DOI: 10.1016/0034-4257(94)90020-5

[86] Gillies RR, Kustas WP, Humes KS. A verification of the 'triangle' method for obtaining surface soil water content and energy fluxes from remote measurements of the normalized difference vegetation index (NDVI) and surface. International Journal of Remote Sensing. 1997;**18**(15):3145-3166. DOI: 10.1080/014311697217026

[87] Tanguy M, Baille A, Gonzalez-Real MM, Lloyd C, Cappelaere B, Kergoat L, et al. A new parameterisation scheme of ground heat flux for land surface flux retrieval from remote sensing information. Journal of Hydrology. 2012;**454-455**:113, 122. DOI: 10.1016/j.jhydrol.2012.06.002

[88] Tang RL, Li ZL, TANG BH. An application of the Ts-VI triangle method with enhanced edges determination for evapotranspiration estimation from MODIS data in arid and semi-arid regions: Implementation and validation. Remote Sensing of Environment. 2010;**114**(3):540-551. DOI: 10.1016/j.rse.2009.10.012

[89] Delogu E, Boulet G, Olioso A, Coudert B, Chirouze J, Ceschia E, et al. Reconstruction of temporal variations of evapotranspiration using instantaneous estimates at the time of satellite overpass. Hydrology and Earth System Sciences. 2012;**16**:2995-3010. DOI: 10.5194/hess-16-2995-2012

[90] Mu Q, Zhao M, Running SW. Improvements to a MODIS global terrestrial evapotranspiration algorithm. Remote Sensing of Environment. 2011;**115**(8):1781-1800. DOI: 10.1016/j.rse.2011.02.019

[91] Baldocchi D, Falge E, Gu L, Olson R, Hollinger D, Running S, et al. FLUXNET: A new tool to study the temporal and spatial variability of ecosystem-scale carbon dioxide, water vapor, and energy flux densities. Bulletin of the American Meteorological Society. 2011;**82**(11):2415-2434. DOI: 10.1175/1520-0477(2001)082<2415:FANTTS>2.3.CO;2

[92] Monteith JL. Solar radiation and productivity in tropical ecosystems. Journal of Applied Ecology. 1972;**9**(3):747-766. DOI: 10.2307/2401901

[93] Mccallum I, Wagner W, Schmullius C. Satellite-based terrestrial production efficiency modelling. Carbon Management. 2009;**4**(8):1-14. DOI: 10.1186/1750-0680-4-8

[94] Tan KP, Kanniah KD, Cracknell AP. A review of remote sensing based productivity models and their suitability for studying oil palm productivity in tropical regions. Progress in Physical Geography. 2012;**9**(5):655-679. DOI: 10.1177/0309133312452187

[95] Potter CS, Randerson JT, Field CB, Matson PA, Vitousek PM, Mooney HA. Terrestrial ecosystem production: A process model-based on global satellite and surface data. Global Biogeochemical Cycles. 1993;**7**(4):811-841. DOI: 10.1029/93GB02725

[96] Potter CS, Klooster SA, Brooks V. Interannual variability in terrestrial net primary production: Exploration of trends and controls on regional to global scales. Ecosystems. 1999;**2**(1):36-48. DOI: 10.1007/s100219900

[97] Zhang LX, Zhou DC, Fan JW, Hu ZM. Comparison of four light use efficiency models for estimating terrestrial gross primary production. Ecological Modelling. 2015;**300**: 30-39. DOI: 10.1016/j.ecolmodel.2015.01.001

[98] Defries RS, Field CB, Fung I, Justice CO, Los S, Matson PA, et al. Mapping the land surface for global atmosphere-biosphere models: Toward continuous distributions of vegetation's functional properties. Journal of Geophysical Research. 1995;**100**(D10):20867-20882. DOI: 10.1029/95JD01536

[99] Nayak RK, Patel NR, Dadhwal VK. Estimation and analysis of terrestrial net primary productivity over India by remote sensing driven terrestrial biosphere model. Environmental Monitoring and Assessment. 2009;**170**(1-4):195-213. DOI: 10.1007/ s10661-009-1226-9

[100] Yu D, Shi P, Shao H. Modelling net primary productivity of terrestrial ecosystems in East Asia based on an improved CASA ecosystem model. International Journal of Remote Sensing. 2009;**30**(18):4851-4866. DOI: 10.1080/01431160802680552

[101] Chhabra A, Dhadwall VK. Estimating terrestrial net primary productivity over India using satellite data. Current Science. 2004;**86**(2):269-271

[102] Verstraeten WW, Veroustraete F, Feyen J. On temperature and water limitation on net ecosystem productivity: Implementation in the C-fix model. Ecological Modeling. 2006;**199**(1):4-22. DOI: 10.1016/j.ecolmodel.2006.06.008

[103] Myneni RB, Williams DL. On the relationship between fAPAR and NDVI. Remote Sensing of Environment. 1994;**49**(3):200-211. DOI: 10.1016/0034-4257(94)90016-7

[104] Mccree KJ. Test of current definitions of photosynthetically active radiation against leaf photosynthesis data. Agricultural Meteorology. 1972;**10**:442-453. DOI: 10.1016 /0002-1571(72)90045-3

[105] Veroustraete F, Patyn J, Myneni RB. Estimating net ecosystem exchange of carbon using the normalised difference vegetation index and an ecosystem model. Remote Sensing of Environment. 1996;**58**(1):115-130. DOI: 10.1016/0034-4257(95)00258-8

[106] Verstraeten WW, Veroustraete F, Wagner W, Van Roey T, Heyns W, Verbeiren S, et al. Remotely sensed soil moisture integration in an ecosystem carbon flux model. The spatial implication. Climatic Change. 2010;**103**(1-2):117-136. DOI: 10.1007/s10584-010-9920-8

[107] Veroustraete F, Sabbe H, Rasse DP, Bertels L. Carbon mass fluxes of forests in Belgium determined with low resolution optical sensors. International Journal of Remote Sensing. 2004;**25**(4):769-792. DOI: 10.1080/0143116031000115238

[108] Xiao XM, Hollinger D, Aber J, Goltz M, Davidson EA, Zhang QY. Satellite-based modeling of gross primary production in an evergreen needleleaf forest. Remote Sensing of Environment. 2004;**89**(4):519-534. DOI: 10.1016/j.rse.2003.11.008

[109] Field CB, Randerson JT, Malmstrom CM. Global net primary production combining ecology and remote sensing. Remote Sensing of Environment. 1995;**5**(1):74-88. DOI: 10.1016/0034-4257(94)00066-V

[110] Huete A, Didan K, Miura T, Rodriguez EP, Gao X, Ferreira LG. Overview of the radiometric and biophysical performance of the MODIS vegetation indices. Remote Sensing of Environment. 2002;**83**(1-2):195-213. DOI: 10.1016/S0034-4257(02)00096-2

[111] Huete AR, Liu HQ, Batchily K, Vanleeuwen W. A comparison of vegetation indices global set of TM images for EOS MODIS. Remote Sensing of Environment. 1997;**59**(3):440-451. DOI: 10.1016/S0034-4257(96)00112-5

[112] Boles S, Xiao X, Zhang Q, Munkhutya S, Liu J, Ojima DS. Land cover characterization of temperate East Asia: Using multi-temporal image data of VEGETATION sensor. Remote Sensing of Environment. 2004;**90**(4):477-489. DOI: 10.1016/j.rse.2004.01.016

[113] Asner GP, Wessman CA, Archer S. Scale dependence of absorption of photosynthetically active radiation in terrestrial ecosystems. Ecological Applications. 1998;**8**(4):1003-1021. DOI: 10.1890/1051-0761(1998)008[1003:SDOAOP]2.0.CO;2

[114] Xiao XM, Zhang QY, Saleska S, Hutyra L, Camargo P, Wofsy S. Satellite-based modeling of gross primary production in a seasonally moist tropical evergreen forest. Remote Sensing of Environment. 2005;**94**(1):105-122. DOI: 10.1016/j.rse.2004.08.015

[115] Liu J, Sun OJ, Jin H, Zhou Z, Han X. Application of two remote sensing GPP algorithms at a semiarid grassland site of North China. Journal of Plant Ecology. 2011;**4**(4):302-312. DOI: 10.1093/jpe/rtr019

[116] Jiang X, Rauscher S, Ringler T, Lawrence D, Williams A, Allen C, et al. Projected future changes in vegetation in western North America in the twenty-first century. Journal of Climate. 2013;**26**:3671-3686. DOI: 10.1175/JCLI-D-12-00430.1

[117] Rahman AF, Sims DA, Cordova VD, El-Masri BZ. Potential of MODIS EVI and surface temperature for directly estimating per-pixel ecosystem C fluxes. Geophysical Research Letters. 2005;**32**(19):1-4. DOI: 10.1029/2005GL024127

[118] Sims DA, Luo H, Hastings S, Oechel WC, Rahmanc AF, Gamon JA. Parallel adjustments in vegetation greenness and ecosystem CO_2 exchange in response to drought in a Southern California chaparral ecosystem. Remote Sensing of Environment. 2006;**103**(3):289-303. DOI: 10.1016/j.rse.2005.01.020

[119] Wu CY, Chen JM, Huang N. Predicting gross primary production from the enhanced vegetation index and photosynthetically active radiation: Evaluation and calibration. Remote Sensing of Environment. 2011;**115**(12):3424-3435. DOI: 10.1016/j.rse.2011.08.006

[120] Leigh EG. Tropical Forest Ecology: A Review from Barro Colorado Island. New York: Oxford University Press; 1999 264 p

[121] Ryu Y, Baldocchi DD, Kobayashi H, Van Ingen C, Li J, Black TA, et al. Integration of MODIS land and atmosphere products with a coupled-process model to estimate gross primary productivity and evapotranspiration from 1 km to global scales. Global Biogeochemical Cycles. 2011;**25**(4):1-24. DOI: 10.1029/2011GB004053

[122] Yang J, Gong P, Fu R, Zhang M, Chen J, Liang S, et al. The role of satellite remote sensing in climate change studies. Nature Climate Change. 2013b;**3**:875-883. DOI: 10.1038/nclimate1908

[123] Martínez B, Gilabert MA. Vegetation dynamics from NDVI time series analysis using the wavelet transform. Remote Sensing of Environment. 2009;**113**(9):1823-1842. DOI: 10.1016/j.rse.2009.04.016

[124] Ghent D, Kaduk J, Remedios J, Balzter H. Data assimilation into land surface models: The implications for climate feedbacks. International Journal of Remote Sensing. 2011;**32**(3):617-632. DOI: 10.1080/01431161.2010.517794

[125] Zhan X, Sohlberg RA, Townshend JRG, Dimiceli C, Carroll ML, Eastman JC, et al. Detection of land cover changes using MODIS 250 m data. Remote Sensing of Environment. 2002;**83**(1-2):336-350. DOI: 10.1016/S0034-4257(02)00081-0

[126] Schaaf C, Gao F, Strahler A, Lucht W, Li X, Tsung T, et al. First operational BRDF, albedo and nadir reflectance products from MODIS. Remote Sensing of Environment. 2002;**83**(1-2):135-148. DOI: 10.1016/S0034-4257(02)00091-3

[127] Wan Z, Zhang Y, Zhang Q, Li ZL. Quality assessment and validation of the MODIS global land surface temperature. International Journal of Remote Sensing. 2004;**25**(1):261-274. DOI: 10.1080/0143116031000116417

[128] Gao X, Huete AR, Ni W, Miura T. Optical-biophysical relationships of vegetation spectra without background contamination. Remote Sensing of Environment. 2000;**74**(3):609-620. DOI: 10.1016/S0034-4257(00)00150-4

[129] Friedl MA, Mciver DK, Hodges JC, Zhang XY, Muchoney D, Strahler AH, et al. Global land cover mapping from MODIS: Algorithms and early results. Remote Sensing of Environment. 2002;**83**(1-2):287-302. DOI: 10.1016/S0034-4257(02)00078-0

[130] Zhao M, Heinsch F, Nemani RR, Running S. Improvements of the MODIS terrestrial gross and net primary production global data set. Remote Sensing of Environment. 2005;**95**(2):164-176. DOI: 10.1016/j.rse.2004.12.011

[131] Comair GF, Mckinney DC, Siegel D. Hydrology of the Jordan River basin: Watershed delineation, precipitation and evapotranspiration. Water Resources Management. 2012;**26**(14):4281-4293. DOI: 10.1007/s11269-012-0144-8

[132] Tang R, Shao K, Li ZL, Wu H, Tang BH, Zhou G. et al, Multiscale validation of the 8-day MOD16 evapotranspiration product using flux data collected in China. IEEE Journal of Selected Topics in Applied Earth Observations and Remote Sensing. 2015;**8**(4):1478-1486. DOI: 10.1109/JSTARS.2015.2420105

[133] Sun Z, Wang Q, Ouyang Z, Watanabe M, Matsushita B, Fukushima T. Evaluation of MOD16 algorithm using MODIS and ground observational data in winter wheat field in North China plain. Hydrological Processes. 2007;**21**(9):1196-1206. DOI: 10.1002/hyp.6679

[134] Running SW, Nemani RR, Heinsch FA, Zhao MS, Reeves M, Hashimoto H. A continuous satellite-derived measure of global terrestrial primary production. Bioscience. 2004;**54**(6):547-560. DOI: 10.1641/0006-3568(2004)054[0547:ACSMOG]2.0.CO;2

[135] Heinsch F, Zhao M, Running SW, Kimball JS, Nemani RR, Davis KJ, et al. Evaluation of remote sensing based terrestrial productivity from MODIS using regional tower eddy flux network observations. IEEE Transactions on Geoscience and Remote Sensing. 2006;**44**(7):1908-1925. DOI: 10.1109/TGRS.2005.853936

[136] Coops NC, Black TA, Jassal RPS, Trofymow JAT, Morgenstern K. Comparison of MODIS, eddy covariance determined and physiologically modeled gross primary production (GPP) in a Douglas-fir forest stand. Remote Sensing of Environment. 2007;**107**(3):385-401. DOI: 10.1016/j.rse.2006.09.010

[137] Wang X, Ma M, Li X, Song Y, Tan J, Huang G, et al. Validation of MODIS-GPP product at 10 flux sites in northern China. International Journal of Remote Sensing. 2013;**34**(2):587-599. DOI: 10.1080/01431161.2012.715774

[138] Zhao M, Running S, Nemani RR. Sensitivity of moderate resolution imaging Spectroradiometer (MODIS) terrestrial primary production to the accuracy of meteorological reanalyses. Journal of Geophysical Research. 2006;**111**(G1):1-13. DOI: 10.1029/2004JG000004

[139] Turner DP, Ritts WD, Cohen WB, Gower ST, Running SW, Zhao M. Evaluation of MODIS NPP and GPP products across multiple biomes. Remote Sensing of Environment. 2006;**102**(3-4):282-292. DOI: 10.1016/j.rse.2006.02.017

[140] Gilabert MA, Moreno A, Maselli F, Martínez B, Chiesi M, Sánchez-Ruiz S, et al. Daily GPP estimates in Mediterranean ecosystems by combining remote sensing and meteorological data. ISPRS Journal of Photogrammetry and Remote Sensing. 2015;**102**:184-197. DOI: 10.1016/j.isprsjprs.2015.01.017

[141] Wu W, Hall CAS, Scatena FN, Quackenbush LJ. Spatial modelling of evapotranspiration in the Luquillo experimental forest of Puerto Rico using remotely-sensed data. Journal of Hydrology. 2006;**328**(3-4):733-752. DOI: 10.1016/j.jhydrol.2006.01.020

[142] Aragao LEOC, Poulter B, Barlow JB, Anderson LO, Malhi Y, Saatchi S, et al. Environmental change and the carbon balance of Amazonian forests. Biological Reviews. 2014;**89**(4):913-931. DOI: 10.1111/brv.12088